# Supporting Information

## Segmentation and Re-encapsulation of Porous PtCu Nanoparticles by Generated Carbon Shell for Enhanced Ethylene-glycol Oxidation and Oxygen-reduction Reaction

Juanjuan Gao [†, ǁ, 1], Mengxi Mao [†, 1], Peiwen Li [†, 1], Rumeng Liu [†, 1], Haiou Song [‡, *], Kuan Sun [§], Shupeng Zhang [†, *]

[†] School of Chemical Engineering, Nanjing University of Science and Technology, Nanjing, 210094, PR China

[‡] School of Environment, Nanjing Normal University, Nanjing, 210097, PR China

[§] MOE Key Laboratory of Low-grade Energy Utilization Technologies and Systems, School of Energy & Power Engineering, Chongqing University, Chongqing 400044, PR China

[ǁ] School of Chemistry and Chemical Engineering, Yancheng Institute of Technology, Yancheng 224051, PR China

[*] Corresponding authors: S.P. Zhang (Email address: shupeng_2006@126.com) and H.O. Song (Email address: songhaiou2011@126.com)

[1] Juanjuan Gao, Mengxi Mao, Peiwen Li and Rumeng Liu contributed equally to this work.

## 1. Experimental

### 1.1. Chemicals and Materials

Potassium tetrachloroplatinate hexahydrate ($K_2PtCl_4 \cdot 6H_2O$), copper chloride dihydrate ($CuCl_2 \cdot 2H_2O$), potassium hydroxide (KOH), L-ascorbic acid (AA), poly(vinylpyrrolidone) (PVP, molecular weight (*Mw* = 40 000), tetraethyl orthosilicate (TEOS, 98.0%), and ethylene glycol (EG) were purchased from Aladdin Chemistry Co., Ltd. Commercial Pt/C (20 wt% of ~ 3 nm Pt NPs on Vulcan XC-72 carbon support) catalyst and Nafion solution (5%) were ordered from Sigma-Aldrich. All other chemicals used in the experiment were analytical grade and used without further purification. All aqueous solutions were prepared with secondary distilled water.

### 1.2. Characterization

The morphology, structure and particle size were characterized using the transmission electron microscope (TEM, JEM-2100HR JEOL) operating at 200 kV and scanning electron microscopy (SEM, S-3400N II) equipped with an energy-dispersive X-ray spectroscopy (EDS, EX-250). The high-resolution TEM (HRTEM) images, selected-area electron diffraction (SAED) and elemental mapping of the final catalyst were further conducted on FE-TEM (FEI Talos F200S G2) with an excellent resolution specification of 0.16 nm in STEM mode. The corresponding characterization samples were prepared through dropping the electrocatalyst suspension dispersed in ethanol on a carbon-coated copper grid.[1] The phase and crystallinity of the samples were recorded on X-ray diffraction (XRD) spectroscope by the Bruker D8 Advance diffractometer with Cu K$\alpha$ radiation. The concentration of final catalyst was determined by the inductively coupled plasma mass spectrometry (ICP-MS, Thermo Scientific iCAP Q).[2, 3] X-ray photoelectron spectroscopy spectra (XPS) were

performed on a PHI Quantera II with a monochromatized Al-kα X-ray source (1486.71 eV photons).[4] Thermo-gravimetric analyses (TGA) were run under $N_2$, between 50 and 800 °C, with a 20 °C/min temperature ramp rate.

### 1.3. Preparation of PtCu NPs.[2]

In a typically synthesized, 1 mL of freshly prepared aqueous solution containing 0.7 mL of 20 mM $K_2PtCl_4$, 0.3 mL of 20 mM $CuCl_2$, and 0.01 g of PVP was quickly added to 1 mL of 0.1 M AA, and then the mixture was sonicated at room temperature for 15 min. Finally, the resulting product was washed three times with ethanol by centrifugation at 11 000 rpm for 15 min, and then dried for stored.

### 1.4. Electrochemical tests

Cyclic voltammogram (CV), linear sweep voltammogram (LSV), electrochemical impedance spectroscopy (EIS), chronoamperometry (i-t) experiments were performed using a CHI 660E electrochemical analyzer (Chenhua Co., Shanghai, China). A conventional three-electrode cell was used, including an Ag/AgCl (3M KCl) electrode as a reference electrode, a Pt wire as a counter electrode, and a working electrode.[2]

### 1.5. Preparation of the catalyst-modified GCE and RDE.

Prior to the surface coating, 4.0 mg of UsPtCu@C catalyst was dispersed in 2 mL water under sonicated for 2 h. Then 6 μL or 10 μL of the resulting suspension was dropped onto a pre-polished glassy carbon electrode (GCE, D = 3 mm) or rotating disk electrode (RDE, S = 0.126 $cm^2$), respectively and dried at ambient conditions. Total metal loading of Pt was controlled in the range of

1.2245 μg for GCE and 2.0408 μg for RDE (based on ICP-MS measurement, 10.204 wt%). Then 3 μL or 5 μL of Nafion (0.05%) was coated on the surface of the modified GCE or RDE, respectively and dried before electrochemical experiments. The intermediate PtCu and commercial Pt/C (20 wt% Pt on Vulcan XC-72) catalyst which were used for the contrast experiment were prepared in the same way.

### 1.6. Ethylene glycol oxidation reaction (EGOR)

The modified GCE was selected as the working electrode and electrochemical measurements were conducted at room temperature. EGOR measurements were performed in a 0.5 M $N_2$-saturated KOH solution containing 1 M EG at a scan rate of 50 mV/s. EGOR durability tests were verified by the accelerated durability test (ADT) of i-t and continuous CV. The former recorded the chronoamperometric stability within 80000 s at a –0.1 V (vs. Ag/AgCl); The latter scan rate was 50 mV/s with cycles from 0 to 5000. And all of the potentials recorded in this part are given with respect to a reversible hydrogen electrode (RHE) by the formula E(RHE) = E(Ag/AgCl) + 0.0591pH + 0.197, and the pH value is measured by a pH meter.

Current densities were normalized in reference to the geometric area of the working electrode, and specific and mass activities were normalized in reference to the electrochemically surface area (ECSA) and loading amount of Pt, respectively. The ECSA of catalyst has been evaluated by CV measurements in $N_2$-saturated 0.5 M $HClO_4$ aqueous solution with a sweep rate of 50 mV/s, and the value of ECSA was estimated by measuring the charge associated with $H_{upd}$ desorption ($Q_H$) between 0.015 and 0.37 V versus RHE, and the specific ECSA was calculated based on the following relation:[5, 6]

$$\mathrm{ECSA} = \frac{Q_H}{m \times q_H} \qquad \text{(S1)}$$

where $Q_H$ is the charge for $H_{upd}$ desorption, $m$ is the Pt loading amount on the electrode and $q_H$ (210 μC/cm$^2$) is the charge required for monolayer desorption of hydrogen on Pt surfaces.

### 1.7. Oxygen reduction reaction (ORR).

To obtain steady state voltammetric data on an RDE, a glass carbon RDE loaded with electrocatalyst was used as the working electrode. The ORR was carried out in an $O_2$ saturated 0.1 M KOH aqueous solution. Prior to each measurement, the electrolyte was bubbled with $O_2$ or $N_2$ until saturation. A constant $O_2$ or $N_2$ flow was then maintained in the headspace of the electrolyte during the whole experiment. The ORR performance was first investigated by CV in $O_2$-saturated 0.1 M KOH at a scan rate of 10 mV/s at room temperature. LSV was performed in the potential range of –0.8 to 0.2 V vs. Ag/AgCl at various rotation rates (400–2400 rpm) in 0.1 M KOH under constant $O_2$ gas flow, with a sweeping rate of 10 mV/s. The durability test for methanol, methanol (3 μL) was added to the $O_2$-saturated 0.1 M KOH aqueous solution around 1000 s, and the current was collected at –0.1 V (vs. Ag/AgCl) with a rotation speed of 1600 rpm. And all of the potentials recorded in this part are given with respect to a reversible hydrogen electrode (RHE) by related calculations.

The kinetic-limiting current ($J_k$) was calculated according to the Koutecky-Levich (K-L) equation:[7]

$$\frac{1}{J} = \frac{1}{J_k} + \frac{1}{J_d} = \frac{1}{J_k} + \frac{1}{B\omega^{1/2}} \qquad \text{(S2)}$$

where J is the experimentally measured current density, $J_d$ is the diffusion-limiting current density and $\omega$ is the angular velocity of electrode rotation. The parameter B can be written as following:[8]

$$B = 0.2nF(D_0)^{2/3}\nu^{-1/6}C_0 \qquad \text{(S3)}$$

F is the Faraday constant (96,485 C/mol), $\nu$ is the kinematic viscosity (0.011 $cm^2/s$) of the aqueous solution, $D_0$ is the diffusion coefficient ($1.93 \times 10^{-5}$ $cm^2/s$) of $O_2$ in 0.1 M KOH aqueous solution, $C_0$ is the bulk concentration of $O_2$ ($1.2 \times 10^{-6}$ $mol/cm^3$) in the electrolyte. $n$ is the number of electrons transferred per $O_2$ and can be calculated from the slope of the K-L plots.[9]

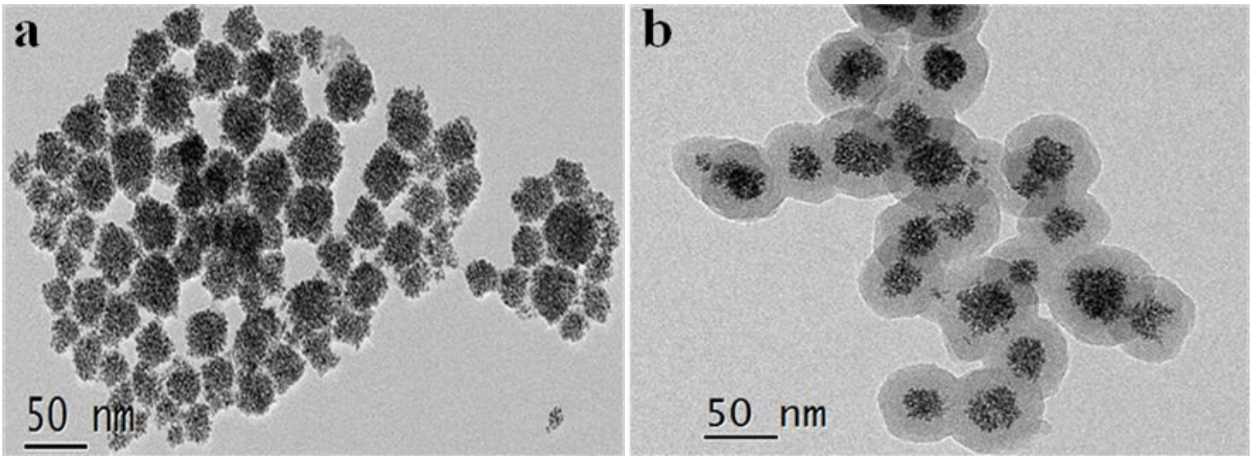


**Fig. S1.** TEM images of PtCu NCs (a) and PtCu@$SiO_2$ core–shell nanospheres (b).

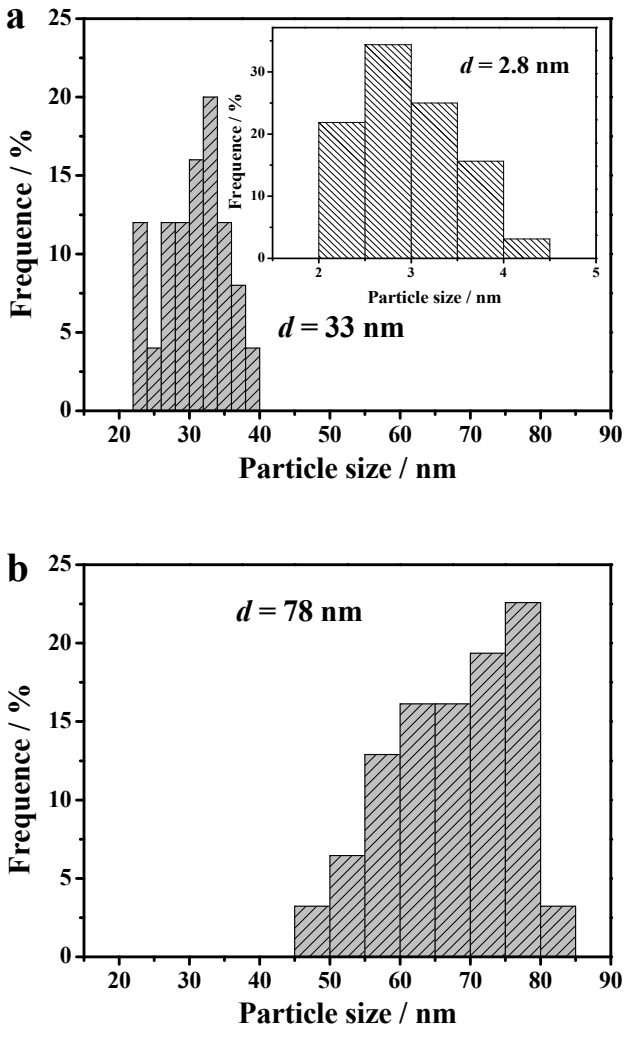

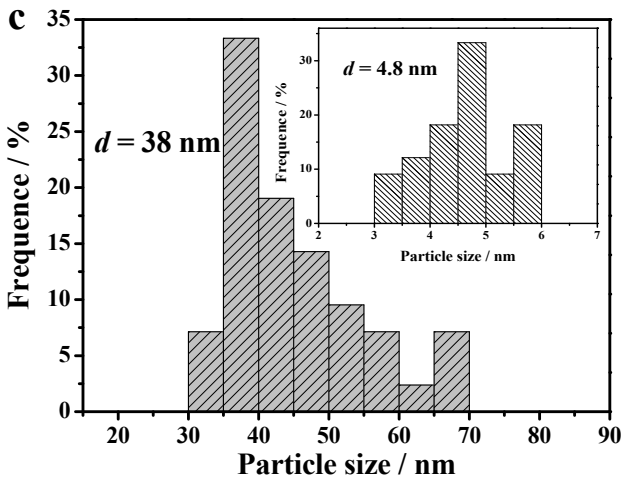


**Fig. S2.** Histograms showing the particle-size distributions of the PtCu NCs (**a**), PtCu@$SiO_2$ core–shell nanospheres (**b**), porous UsPtCu@C nanostructures (**c**). The insets in (**a**) and (**c**) display the corresponding particle size distribution of interconnected arms, respectively.

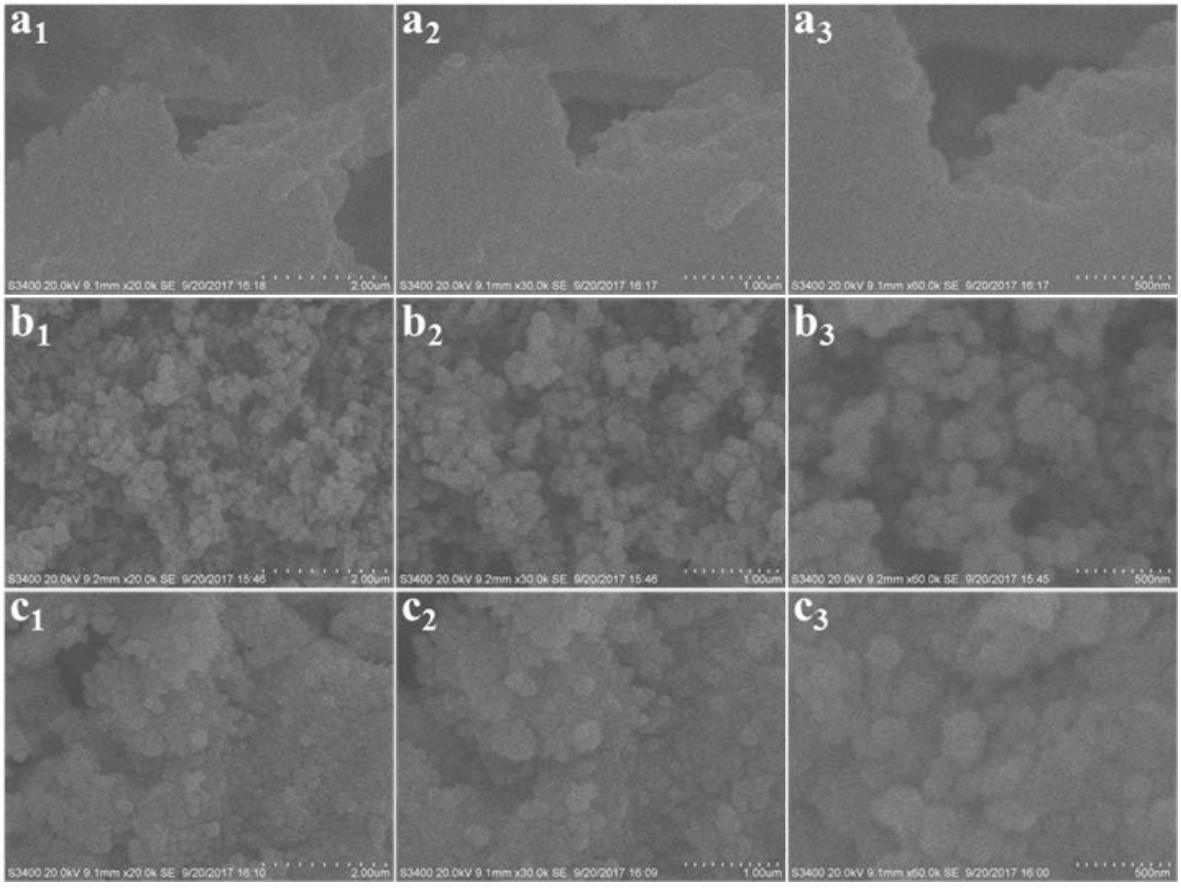


**Fig. S3.** Different-magnification SEM images of PtCu NCs (**a**$_1$–**a**$_3$), PtCu@$SiO_2$ core–shell nanospheres (**b**$_1$–**b**$_3$), porous UsPtCu@C nanostructures (**c**$_1$–**c**$_3$).

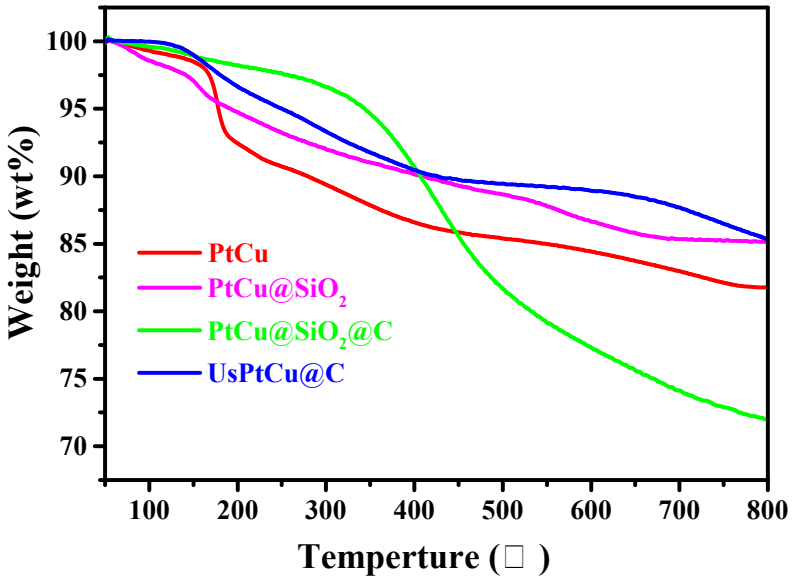


**Fig. S4.** Thermo-gravimetric analysis (TGA) curves of PtCu, PtCu@$SiO_2$, PtCu@$SiO_2$@C and UsPtCu@C.

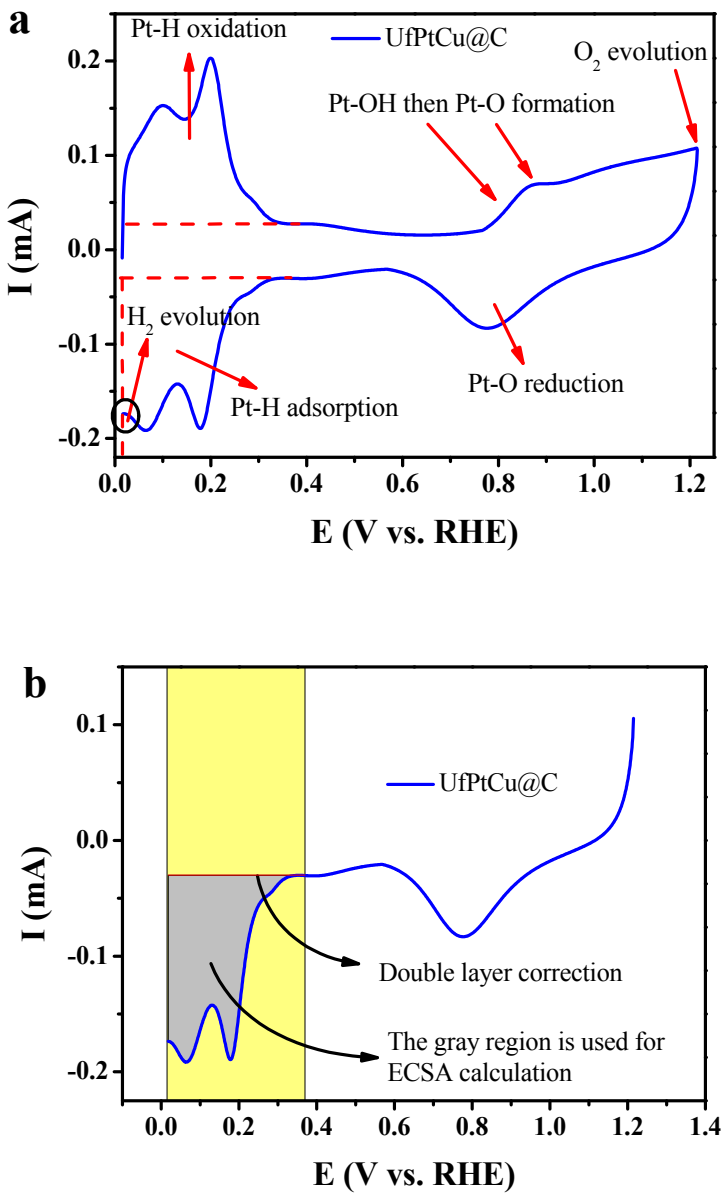


**Fig. S5.** (**a**) CV of UsPtCu@C in $N_2$-saturated 0.5 M $HClO_4$ aqueous solution, the potential region of from 0.015 to 1.215 V versus RHE, with a scan rate of 50 mV/s. (**b**) gray region is used to calculate the ECSA for UsPtCu@C.

**References**


(1) Lee, Y. W.; Hwang, E. T.; Kwak, D. H.; Park, K. W. Preparation and Characterization of PtIr Alloy Dendritic Nanostructures with Superior Electrochemical Activity and Stability in Oxygen Reduction and Ethanol Oxidation Reactions. *Catal. Sci. Technol.* **2016**, *6* (2), 569–576.

(2) Eid, K.; Wang, H.; He, P.; Wang, K.; Ahamad, T.; Alshehri, S. M.; Yamauchi, Y.; Wang, L. One–Step Synthesis of Porous Bimetallic PtCu Nanocrystals with High Electrocatalytic Activity for Methanol Oxidation Reaction. *Nanoscale* **2015**, *7* (40), 16860–16866.

(3) Wang, J.; Chen, F.; Jin, Y.; Lei, Y.; Johnston, R. L. One-Pot Synthesis of Dealloyed AuNi Nanodendrite as a Bifunctional Electrocatalyst for Oxygen Reduction and Borohydride Oxidation Reaction. *Adv. Funct. Mater.* **2017**, *27* (23), 1700260.

(4) Zhang, N.; Bu, L.; Guo, S.; Guo, J.; Huang, X. Screw Thread–Like Platinum–Copper Nanowires Bounded with High–Index Facets for Efficient Electrocatalysis. *Nano Lett.* **2016**, *16* (8), 5037–5043.

(5) He, D.; Zhang, L.; He, D.; Gang, Z.; Yue, L.; Deng, Z.; Xun, H.; Wu, Y.; Chen, C.; Li, Y. Amorphous Nickel Boride Membrane on a Platinum–Nickel Alloy Surface for Enhanced Oxygen Reduction Reaction. *Nat. Commun.* **2016**, *7*, 12362.

(6) Lu, S.; Eid, K.; Lin, M.; Wang, L.; Wang, H.; Gu, H. Hydrogen Gas–Assisted Synthesis of Worm–Like PtMo Wavy Nanowires as Efficient Catalysts for the Methanol Oxidation Reaction. *J. Mater. Chem. A* **2016**, *4* (27), 10508–10503.

(7) Yu, H.; Shang, L.; Bian, T.; Shi, R.; Waterhouse, G. I. N.; Zhao, Y.; Zhou, C.; Wu, L. Z.; Tung, C. H.; Zhang, T. Carbon Nanosheets: Nitrogen-Doped Porous Carbon Nanosheets Templated from g-$C_3N_4$ as Metal-Free Electrocatalysts for Efficient Oxygen Reduction Reaction. *Adv. Mater.* **2016**, *28* (25), 5140–5140.

(8) Xia, T.; Liu, J.; Wang, S.; Wang, C.; Sun, Y.; Gu, L.; Wang, R. Enhanced Catalytic Activities of NiPt Truncated Octahedral Nanoparticles toward Ethylene Glycol Oxidation and Oxygen Reduction

in Alkaline Electrolyte. *ACS Appl. Mater. Interfaces* **2016**, *8* (17), 10841–10849.

(9) Nandan, R.; Nanda, K. K. A Unique Approach in Designing Resilient Bi–Functional Nano–Electrocatalysts Based on Ultrafine Bimetallic Nanoparticles Dispersed in Carbon Nanospheres. *J. Mater. Chem. A* **2017**, *5* (21), 10544–10553.